Distribution of a Putative Cell Surface Receptor for Fibronectin and Laminin in the Avian Embryo

Danuta M. Krotoski, Carmen Domingo, and Marianne Bronner-Fraser

Developmental Biology Center and Department of Developmental and Cell Biology,
University of California, Irvine, California 92717

Abstract. The cell substratum attachment (CSAT) antibody recognizes a 140-kD cell surface receptor complex involved in adhesion to fibronectin (FN) and laminin (LM) (Horwitz, A., K. Duggan, R. Greggs, C. Decker, and C. Buck, 1985, *J. Cell Biol.*, 101:2134–2144). Here, we describe the distribution of the CSAT antigen along with FN and LM in the early avian embryo. At the light microscopic level, the staining patterns for the CSAT receptor and the extracellular matrix molecules to which it binds were largely codistributed. The CSAT antigen was observed on numerous tissues during gastrulation, neurulation, and neural crest migration: for example, the surface of neural crest cells and the basal surface of epithelial tissues such as the ectoderm, neural tube, notochord, and dermomyotome. FN and LM immunoreactivity was observed in the basement membranes surrounding many of these epithelial tissues, as well as around the otic and optic vesicles. In addition, the pathways followed by cranial neural crest cells were lined with FN and LM. In the trunk region, FN and LM were observed surrounding a subpopulation of neural crest cells. However, neither molecule exhibited the selective distribution pattern necessary for a guiding role in trunk neural crest migration. The levels of CSAT, FN, and LM are dynamic in the embryo, perhaps reflecting that the balance of surface–substratum adhesions contributes to initiation, migration, and localization of some neural crest cell populations.

INTERACTIONS between the cell surface and the extracellular matrix (ECM)[1] have been proposed to be important for many aspects of embryonic development including cell growth, cell migration, and cell differentiation (cf. 20). Many ECM components have been identified in regions undergoing morphogenesis and have been suggested to promote cell migration. For example, fibronectin (FN) has been implicated in guiding cell movement during gastrulation and neural crest migration (5, 41), laminin (LM) has been suggested to promote neurite outgrowth (29, 46, 47), and hyaluronate may facilitate cell migration (55, 57).

FN and LM are two ECM components that appear to have a wide variety of functions in cell adhesion and motility (for reviews see references 24, 25, 50, and 54). Both molecules are glycoproteins but are distinct with respect to structure, function, and mechanisms of adhesion (49, 51). FN promotes attachment and spreading of some cell types, influences cytoskeletal organization and cell migration, is involved in hemostasis, and is altered in oncogenic transformation (24). In the embryo, FN appears to line some of the pathways followed by migrating cells during gastrulation (2, 30), primordial germ cell migration (21), and neural crest cell migration

(14, 27, 34, 41). LM also influences attachment and spreading of some cell types. In vitro, LM influences the growth (52), morphology (42, 51), and migration (35) of corneal epithelia, epidermal, and nerve cells, among other cell types. Neurons readily attach to and send out axons on LM substrates in vitro; therefore it has been proposed that LM is important for neurite outgrowth and extension in both the peripheral and central nervous system (29, 33, 46). Neural crest cells in vitro also migrate avidly on LM with no apparent preference for FN over LM (17, 39).

Until recently little has been known about the cellular sites to which ECM molecules bind. The isolation of monoclonal antibodies and peptides that inhibit the binding of cells to tissue culture substrates has resulted in the identification of putative cellular receptors for FN (8, 18, 38, 44) and LM (22, 31, 32, 37, 52). The monoclonal antibodies cell substratum attachment (CSAT) (38) and JG22 (14) both recognize a cell surface complex in the molecular mass range of 140 kD (11, 26). The cell surface localization of CSAT and JG22 correlates with that of FN in cultured cells, codistributing around adhesion plaques and in areas of cell–cell contact in migrating fibroblasts (9, 12). The CSAT receptor codistributes with actin along stress fibers (10). On migratory cells such as neural crest cells and somite cells, the distribution of the receptor complex appears to be diffuse and uniform (13). Antibodies to the receptor complex can themselves mediate cell

---

adhesion and spreading when adsorbed to substrata (10, 13). Recent evidence suggests that the CSAT receptor is an integral membrane protein that binds to talin on the cytoplasmic side of the membrane (23). These observations suggest a possible cellular role for the CSAT receptor as a part of a cell surface linkage between FN and the cytoskeleton. In addition to having the ability to bind FN, CSAT is thought to bind LM (22). Furthermore, antibodies to the 140-kD complex affect adhesion of neural crest cells to both FN (3, 13) and LM substrates (4). These results indicate that CSAT may be a multifunctional receptor.

Recent experiments have used CSAT or JG22 antibodies in vivo to test the possible role of the receptor for FN and LM during morphogenesis. Injection of either JG22 (4) or CSAT (6) antibodies caused profound alterations in cranial neural crest migration, including inhibition of migration and ectopic accumulations of neural crest cells. These results suggest that the CSAT antigen may play an important functional role during the migration of cranial neural crest cells. Therefore, a detailed analysis of CSAT localization is necessary to clarify the possible role of this receptor in normal neural crest development.

Here, we have analyzed the distribution of the CSAT antigen in early avian embryos. We have compared the CSAT distribution with that of FN and LM to determine possible correlations between this cell surface molecule and the ECM components to which it is thought to bind. The results confirm and extend previous studies from this (4) and other (13) laboratories to indicate that the CSAT antigen is present on the surface of neural crest cells and many epithelial tissues. Furthermore, CSAT often codistributes with FN and LM, although no obligate correlation between these three molecules could be discerned.

Materials and Methods

Experimental Animals

White Leghorn chick embryos, incubated at 38°C for 1.5–3.5 d and harvested at Hamburger and Hamilton stages 8–25 (19), were used throughout this experiment. The embryos were fixed at the following stages: stages 8–10 for gastrulation and neurulation, stage 10–16 for the cranial neural crest migration and optic and otic vesicle development, stages 11–18 for trunk neural crest migration, and stages 20–25 for formation of neural crest–derived ganglia.

Hybridoma Cells

CSAT hybridoma cells were a generous gift from Dr. Alan F. Horwitz (University of Pennsylvania, Philadelphia, PA). JG22 hybridoma cells were kindly provided by Dr. David Gottlieb (Washington University, St. Louis, MO). The cells were maintained in 75- or 250-ml tissue culture flasks in Dulbecco's modified Eagle's medium containing 15% fetal bovine serum in a 5% CO_2 atmosphere.

Histological Procedures

Cryostat Sections. Embryos were fixed in absolute ethanol or methanol for 48 h at 4°C. They were rehydrated in cold PBS, placed into PBS containing 5% sucrose, 0.01% azide for 2–4 h, and then into 15% sucrose in PBS overnight at 4°C. They were infiltrated with 7.5% gelatin/15% sucrose in PBS at 37°C for 3 h, oriented and frozen in OCT (Miles Laboratories Inc., Naperville, IL) in liquid nitrogen. These fixation and embedding methods were used because they gave optimal antigen preservation and morphology of the embryonic specimens. 15-μm frozen sections were cut on a Histostat Cryostat (Reichardt Scientific Instruments, Buffalo, NY).

Paraffin Sections. To confirm that the observed distribution patterns of FN and LM were not an artifact resulting from the histological techniques

used in this study, we used various fixation and embedding procedures, in addition to frozen sections. Embryos were fixed for 2 h in Zenker's fixative or 10% phosphate-buffered formalin. They were then dehydrated through serial alcohols and embedded in paraplast. Serial 10-μm sections were cut on a microtome (E. Leitz, Inc., Rockleigh, NJ). Though the levels of immunofluorescence were lower in paraffin than in cryostat sections, similar distributions were noted for both FN and LM. CSAT and JG22 antigens were not preserved by these procedures.

Immunofluorescence

Adjacent sections were individually incubated with antibodies against the 140-kD receptor complex (CSAT or JG22), or with antibodies to chicken FN or LM (gifts of Dr. D. Fambrough, Johns Hopkins University, Baltimore, MD). CSAT and JG22 antibodies yielded similar staining patterns. Because CSAT antibodies gave more intense staining, most immunofluorescence was performed with this antibody. For some experiments, sections were double-labeled with either CSAT or JG22 antibodies together with the HNK-1 antibody, which distinguishes migrating neural crest cells (56).

Sections were collected on gelatin-coated slides and air-dried. They were then incubated with culture medium from hybridoma cells (CSAT or JG22) or with purified antibodies (anti-fibronectin, anti-laminin, or anti-CSAT) diluted in PBS containing 0.5% BSA (PBS/BSA) for 2 h at room temperature. For some sections in each series, goat serum (diluted 1:30) was added as a nonimmune control. After washing with PBS/BSA, the slides were incubated with a solution of fluorescein isothiocyanate–conjugated goat anti–mouse IgG (Antibodies, Inc., Davis, CA) diluted 1:300 in PBS/BSA for 45 min at room temperature. HNK-1 staining was performed as described previously (4, 5). Sections were incubated with culture medium supernatant from HNK-1 hybridoma cells for 3 h, rinsed, incubated with rabbit antibodies against mouse IgMs for 1 h, followed by a 1-h incubation with rhodamine isothiocyanate–conjugated goat antibodies against rabbit IgGs. After washing in PBS the slides were mounted in carbonate-buffered glycerol and examined with a Zeiss microscope equipped with epifluorescence optics. Data were recorded photographically and on videotape using a silicon intensifying target image–intensifying video camera (RCA, RCA New Products Div., Lancaster, PA) and a video recorder.

Identification of Antigens

Immunoprecipitation of Labeled Antigens. The molecular specificity of the monoclonal antibodies against FN and LM was determined in whole chicken embryos. The specificity of CSAT in chicken embryos has been reported previously by Knudsen et al. (26).

The specificity of the antibody against chicken LM was determined by immunoprecipitation, according to the method of Brower et al. (7). 2.5-d-old chicken embryos were labeled for 24 h with [^{35}S]methionine (>800 Ci/mmol; New England Nuclear, Boston, MA). The vitelline membrane was removed with a fine needle and 40 μl of labeled methionine was pipetted directly onto the embryo. The eggs were sealed with adhesive tape and incubated for 24 h. They were then dissected from the surrounding membranes and homogenized in lysis buffer (20 mM Tris [pH 8.1], 150 mM NaCl, 1 mM $MgCl_2$, 1 mM $CaCl_2$, 0.5% Nonidet P-40, 0.5% BSA, 1 mM phenylmethylsulfonyl fluoride, 0.5 μg/ml antipapain, 0.5 μg/ml leupeptin, 0.5 μg/ml pepstatin, and 0.1% NaN_3). Embryo homogenate was preabsorbed with protein A sepharose (Sigma Chemical Co., St. Louis, MO) and then incubated with antibodies against chick laminin (20 μg/ml). Protein A sepharose was added to the antibody–antigen mixture overnight and the beads were pelleted in a microfuge. The protein A sepharose beads were washed with Tris saline and eluted with elution buffer (0.1 M citrate [pH 3.0], 100 mM NaCl, 1 mM $MgCl_2$, 1 mM $CaCl_2$, 0.2% Nonidet P-40, and 0.1% NaN_3).

The molecular specificity of the antibody against FN was determined by immunoblotting (16). 2.5-d chicken embryos were homogenized in solubilization buffer (150 mM Tris, 1.5 mM EDTA, and 22% sucrose-containing protease inhibitors). Aliquots of ~50 μg were used for each lane.

Analysis of Antigens by SDS PAGE. SDS PAGE was carried out on 1.5-mm-thick 5–15% gradient running gels with 4% stacking gels using the buffer system of Laemmli (28). Whole chick homogenates (for Western blots) or immunoprecipitates were prepared for electrophoresis by addition of concentrated sample buffer, to yield a final concentration of 4% SDS, 10% glycerol, 0.125 M Tris-HCl (pH 6.8), and 5% β-mercaptoethanol. Samples were boiled for 5 min.

Visualization of Gel Bands. After electrophoresis, gels were fixed and stained with Coomassie Brilliant Blue. Bands labeled with LM were detected by impregnating the gels with Enhance (DuPont Co., Wilmington,

DE), then exposing the dried gels to Kodak XAR film at −80°C. For immunoblots, the proteins were electroeluted onto nitrocellulose and the filters were incubated with the monoclonal antibody against FN (10 μg/ml). Bands were visualized with an alkaline phosphatase second antibody (Promega Biotec, Madison, WI). Apparent molecular mass was estimated by comparison with heavy molecular mass standards (Bethesda Research Laboratories, Gaithersburg, MD).

Results

The localization of the CSAT antigen, together with FN and LM, in early chick embryos is presented below. First, we describe the distribution pattern of CSAT, FN, and LM in gastrulating and neurulating embryos. Then, the distribution of these antigens are described in the cranial and trunk regions both during and after neural crest migration.

CSAT, FN, and LM during Primitive Streak Formation

CSAT. In regions undergoing gastrulation, faint CSAT immunoreactivity was observed outlining the circumference of most cells in the embryo. The CSAT immunofluorescence was more intense on the basal surface of the epiblast (Fig. 1 A), except at the level of Hensen's node, where CSAT immunoreactivity was comparable with that surrounding other cells within the embryo. In addition, many extraembryonic membranes exhibited bright immunofluorescence of constant intensity throughout the developmental stages examined.

FN. In gastrulating embryos, FN immunofluorescence was observed both under the hypoblast and along the basement membrane of the epiblast (Fig. 1 B). This is distinct from the distribution of CSAT, which was observed primarily under the epiblast. At the level of Hensen's node, FN staining was not seen in the basal lamina surrounding the node, though fibrillar FN was observed within the node itself. With the exception of the nodal region which had fibrillar staining, FN was only detected in organized basement membranes.

LM. LM in the gastrulating embryo was observed in the basement membranes surrounding tissues whose cells were outlined by CSAT. LM staining was seen on the basal surface of the epiblast, but was absent from the hypoblast (Fig. 1 C). At the level of Hensen's node, LM was observed within the node itself. LM was only seen in an organized basement membrane except in the nodal region, where the staining appeared fibrillar.

CSAT, FN, and LM during Neurulation

CSAT. After gastrulation and notochord formation, CSAT immunoreactivity was most intense along the basal surface of the neural folds and presumptive neural tube, ectoderm, and notochord. After neural tube closure in the mesencephalon, premigratory neural crest cells residing in the dorsal aspect of the tube could be distinguished from other neural tube cells by their rounded morphology and their position in the neural tube. Both premigratory cranial neural crest cells and other cells within the neural tube, were outlined by CSAT (Fig. 2 A). In the trunk region as well, all neural tube cells were outlined with CSAT, though no morphological distinctions were apparent between neural tube cells and premigratory neural crest cells. In addition to premigratory cells, migrating neural crest cells had CSAT immunoreac-
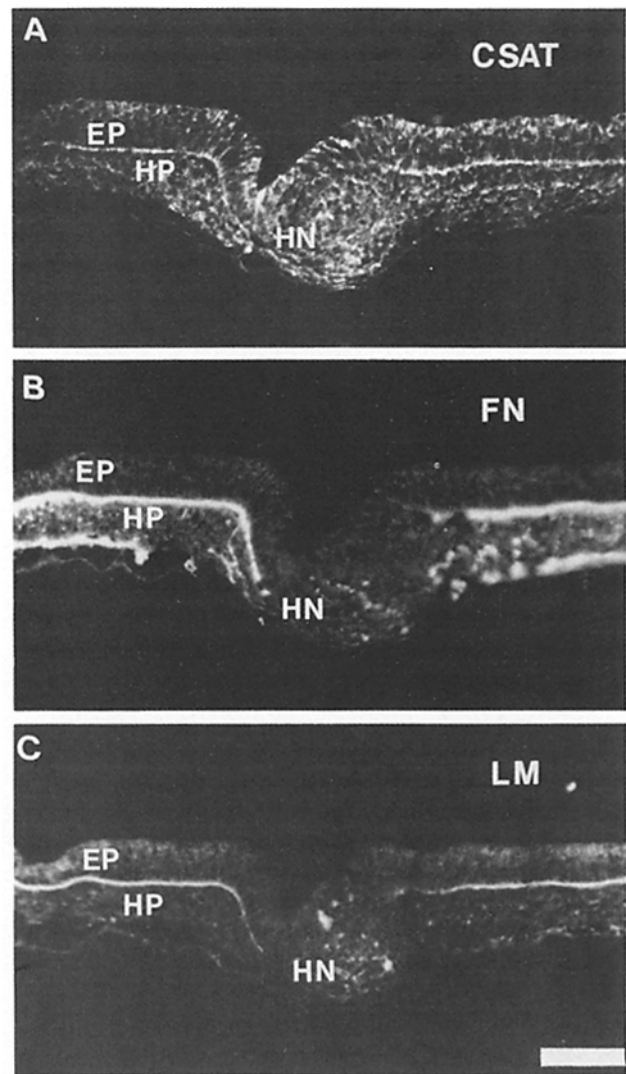
Figure 1. Fluorescence photomicrographs of transverse sections showing *CSAT*, *FN*, and *LM* immunoreactivity in gastrulating regions of chick embryos (stages 8–10) at the level of the Hensen's node (*HN*). (*A*) CSAT immunoreactivity was observed outlining all cells of the embryo, but was particularly noticable on the basal surface of the epiblast (EP). (*B*) FN immunoreactivity was observed on the basal surface of the epiblast and the hypoblast (*HP*). In addition, some punctate staining was seen in Hensen's node. (*C*) LM immunoreactivity was observed on the basal surface of the hypoblast as well as within Hensen's node. Bar, 33 μm.

tivity. CSAT immunofluorescence was also observed around the dorsal aorta.

FN. The FN immunoreactivity during and after neurulation paralleled that of CSAT and was similar to that described by previous investigators (14, 41). For example, fibrillar FN immunoreactivity was detectable in the region surrounding premigratory cranial neural crest cells (Fig. 2 B), which had CSAT immunoreactivity on their surfaces.

LM. The distribution of LM at neurulation was virtually identical to that of FN, with intense staining around the basal surfaces of the neural folds, ectoderm, notochord, and endoderm. In the mesencephalon, LM was detectable in the matrix surrounding the premigratory neural crest cells (Fig. 2 C). In the trunk, LM was seen in the thin matrix between
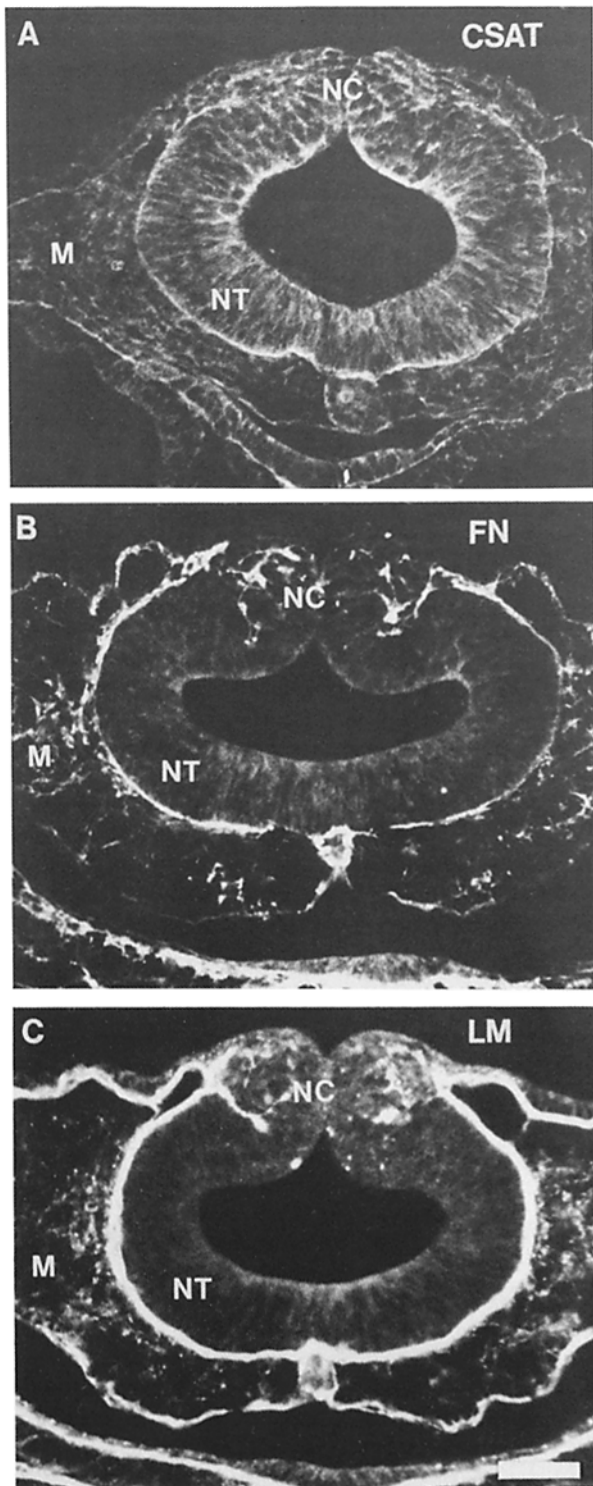
Figure 2. Fluorescence photomicrographs of transverse sections showing *CSAT, FN,* and *LM* immunoreactivity in the mesencephalon just before cranial neural crest migration in stage 10 embryos *(A) CSAT* was observed surrounding most cells in the embryo. Immunoreactivity was particularly noticable around cells of the neural tube *(NT)* including the premigratory neural crest cells *(NC)* that were in the dorsal portion of the neural tube. *(B) FN* was observed on the basal surface of the neural tube, ectoderm, notochord, and endoderm, as well as within the cranial mesenchyme *(M).* FN immunoreactivity was also seen in the area surrounding the premigratory neural crest cells. *(C) LM* immunoreactivity was observed on the basal surface of the neural tube, ectoderm, endoderm, and

the dorsal neural tube and ectoderm that will be invaded by early migrating neural crest cells. This distribution pattern parallels that of FN (14, 41).

CSAT, FN, and LM in the Cranial Region

CSAT. The CSAT staining pattern was similar in the mesencephalon, prosencephalon, and rhombencephalon. CSAT immunofluorescence was observed on the basal surface of the neural tube and ectoderm, as well as surrounding individual cells within the neural tube, notochord, and ectoderm (Fig. 2 *A*). The antigen was also detected around the pharynx and the dorsal and ventral aortae. Before neural crest migration, the head mesenchyme had only low levels of CSAT staining, with the exception of cells lateral to the edges of the pharynx, where immunoreactivity was stronger. As noted in previous studies (4, 13), CSAT was observed on the surface of migrating neural crest cells in the mesencephalon, prosencephalon, and rhombencephalon. In the prosencephalon, CSAT was observed at the basolateral surface of the developing optic vesicle and surrounding individual cells within the vesicle (Fig. 3 *A*). After lens differentiation, CSAT was observed surrounding individual cells in the lens, optic cup, and neural tube, though the intensity of staining was not as high as that observed in the head mesenchyme (Fig. 3 *D*). At the level of the otic vesicle in the rhombencephalon, CSAT immunoreactivity was observed around individual cells of the otic vesicles. Immunoreactivity appeared to be particularly concentrated at the basolateral surface of the otic vesicle (Fig. 4 *A*). With further development, the CSAT immunoreactivity in the cranial region increased around the neural tube, notochord, ectoderm, and neural crest–derived ganglia.

FN. FN immunofluorescence in the head essentially appeared as described elsewhere (13, 14). FN was detected around the entire neural tube, under the ectoderm, around the basal lamina of the foregut, and within the head mesenchyme (Fig. 2 *B*). In addition, FN was observed outlining the optic vesicle shortly after evagination (Fig. 3 *B*). After lens differentiation, FN was seen surrounding the basal surface of the lens and in the head mesenchyme surrounding the optic cup (Fig. 3 *E*). In the rhombencephalon, low levels of FN immunofluorescence were observed surrounding the otic vesicles (Fig. 4 *B*). The distribution of FN in the head largely paralleled that of CSAT.

LM. In the head mesenchyme, striking laminin immunofluorescence was detected around the entire neural tube, under the ectoderm, as well as around the basal lamina of the foregut (Fig. 2 *C*). LM was observed throughout the head mesenchyme, and was most noticeable along the lateral edges. LM immunoreactivity was particularly strong on the basal surface of the otic (Fig. 4 *C*) and optic vesicles (Fig. 3 *C*) and around the optic cup and lens (Fig. 3 *F*). The distribution of LM in the cranial region was similar to that of FN described above, except that LM immunofluorescence appeared continuous along the basal surface of epithelia, whereas FN staining appeared more patchy. In addition, LM immunoreactivity was strong around the basal portion of the optic cup, whereas FN immunoreactivity was weak or absent

notochord. LM was also seen within the cranial mesenchyme and surrounding the premigratory neural crest cells. Bar, 33 µm.

Figure 3. Fluorescence photomicrographs of transverse sections through the prosencephalon of stage 10 (*A–C*) and stage 15 (*D–F*) chicken embryos showing the distribution of *CSAT*, *FN*, and *LM*. (*A*) After the optic vesicle buds off from the neural tube, CSAT staining is observed on the basolateral surface of the neural tube (*NT*) and optic vesicle (*OT*) as well as surrounding individual cells in these structures and in the head mesenchyme. (*B*) FN immunoreactivity was observed on the basolateral surface of the neural tube, optic vesicle, and ectoderm as well as within the head mesenchyme. (*C*) LM immunoreactivity in stage 10 embryos was also observed on the basolateral surface of the neural tube, optic vesicle, and ectoderm as well as within the head mesenchyme. (*D*) In stage 15 embryos, CSAT was observed surrounding cells of the lens, optic cup, and neural tube; marked CSAT immunoreactivity was also observed in the head mesenchyme. (*E*) FN immunoreactivity in stage 15 embryos was strong in the head mesenchyme and surrounding the lens. (*F*) LM immunoreactivity in stage 15 embryos was observed on the basolateral surface of the optic cup, lens, and neural tube. Some LM was also noted in the head mesenchyme. Bars, 100 μm.

on the basolateral surface. The distribution of LM in the head largely paralleled that of CSAT.

In contrast to the sections stained with antibodies against CSAT, FN, or LM, only low levels of background staining were observed in control sections (Fig. 4 *D*) that were stained with nonimmune serum.

CSAT, FN, and LM during Trunk Neural Crest Migration

In the trunk region of avian embryos, neurulation occurs as an anterior to posterior wave. Therefore, numerous stages of neural crest migration occur simultaneously within the same animal; migration is well advanced in anterior regions while just beginning in more posterior regions. Neural crest cells begin their migration shortly after formation of the somites. The somites are epithelial spheres surrounding a core of mesodermal cells, which form by separating from the unsegmented mesenchyme. With increasing embryonic age, the somites dissociate to form the dermomyotome, derived from the dorsolateral somite, and sclerotome, derived from the ventromedial somite.

CSAT. In the trunk, CSAT staining was seen around the neural tube and notochord. Before segmentation, CSAT outlined the periphery of the unsegmented mesenchyme but was only present at low levels surrounding cells within the

mesenchyme. After segmentation, the somites had a low degree of CSAT staining on their basal and apical surfaces and around a few mesenchymal cells within the lumen. After dissociation of the epithelial somites, high levels of CSAT immunoreactivity were observed around the dermomyotome while lesser amounts were detectable around cells of the sclerotome (Figs. 5 *A* and 6 *A*). Subsequently, CSAT fluorescence was visible surrounding individual cells, presumably neural crest cells, in the anterior half of the sclerotome (Figs. 5 *D* and 6 *D*). In contrast, only low levels of CSAT staining were detected in the posterior half of the sclerotome. Neural crest cells invade the anterior half of the somite, while the posterior half is devoid of neural crest cells (5, 45). In sections that were double-labeled with CSAT and HNK-1 antibodies, all HNK-1 positive cells also possessed CSAT immunofluorescence. Since HNK-1 recognizes migrating neural crest cells, this suggests that the cells within the anterior half of the sclerotome with intense CSAT staining were neural crest cells. The CSAT immunoreactivity of the neural crest cell surface was more intense than that on sclerotomal cells. CSAT immunoreactivity was also observed on the intermediate mesoderm along the entire length of the embryo, around the dorsal aorta, the mesonephros, the anterior cardinal vein, the intestines, and extraembryonic membranes. The intensity of CSAT immunoreactivity appeared to increase with age. Consequently, the intensity of CSAT immunostain-

ing appeared somewhat graded along the anterioposterior axis such that more intense staining was observed in the more mature anterior regions.
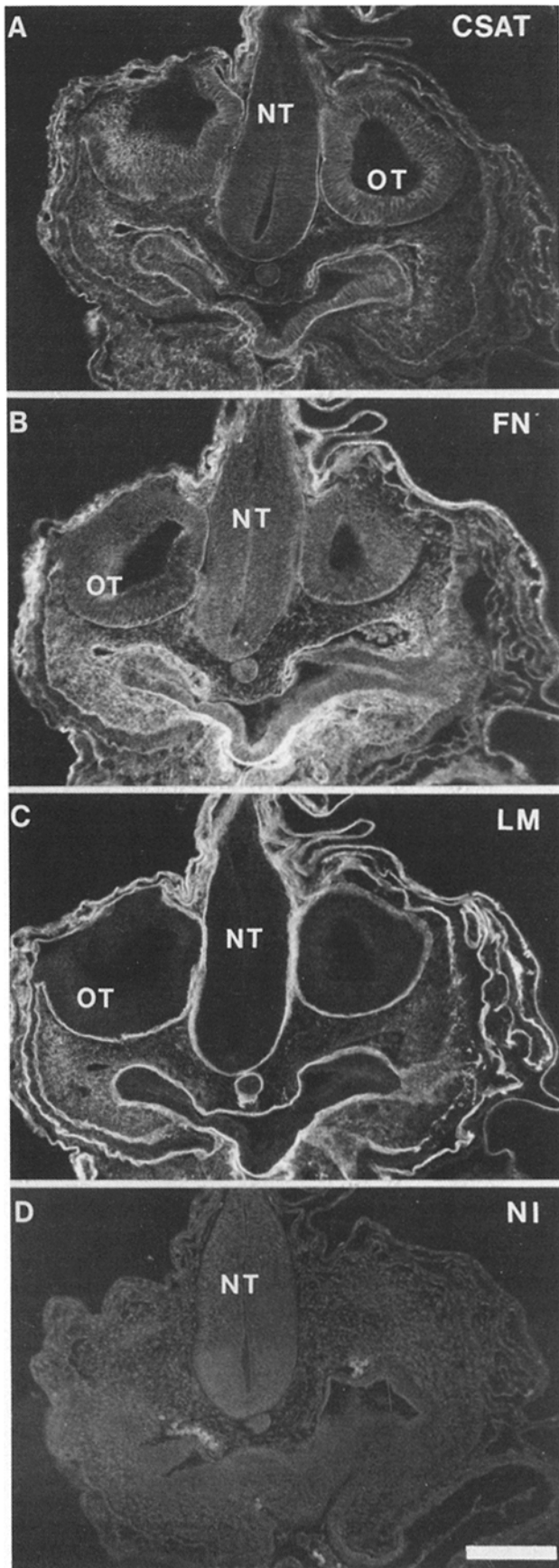
FN. FN reactivity in the trunk was essentially similar to that described by previous investigators (41, 53) with the exception of that surrounding the neural tube. We observed much lower FN immunofluorescence on the ventral surface of the neural tube than on the dorsal surface of the neural tube. In contrast, previous studies using polyclonal antibodies detected FN surrounding the entire neural tube (13, 41). However, in a recent study by Rogers et al. (47), FN immunofluorescence similar to that observed by us was noted around the neural tube.

In the sclerotome, the distribution of CSAT and FN did not entirely overlap. In contrast to CSAT, which was predominantly observed in the anterior half of the sclerotome on the surface of migrating neural crest cells, the levels of fibronectin immunoreactivity were comparable within both anterior and posterior halves of the sclerotome (Figs. 5 *B* and 6 *B*). In double-labeling experiments using HNK-1 to recognize neural crest cells together with antibodies against FN, some but not all HNK-1 positive cells were surrounded by detectable FN immunoreactivity. The sclerotomal FN appeared fibrillar and was of lower intensity than that observed surrounding epithelial tissues (Figs. 5 *B* and 6 *B*). The intensity of FN immunoreactivity in the sclerotome appeared to decrease somewhat during the time that neural crest cells were observed within the somites compared with either earlier or later stages (5e, 6e).

LM. The distribution of laminin in the trunk was similar to that of FN. LM was seen surrounding the notochord, ectoderm, mesonephric tubules, and the neural tube (Figs. 5 *C* and 6 *C*). Before somite formation, no LM immunofluorescence was detected within the unsegmented mesenchyme. After segmentation, LM staining surrounded the epithelial somites, but was not present within the somite. As the somites dissociated to form the dermomyotome and sclerotome, LM immunofluorescence surrounded the dermomyotome (Figs. 5 *F* and 6 *F*). Analogous to the FN distribution, LM immunofluorescence was uniform in the anterior and posterior halves of sclerotome (Figs. 5 *F* and 6 *F*).

Two differences were noted between the staining patterns for FN and LM. First, uniform LM immunofluorescence was seen around the entire basal lamina of the neural tube, whereas FN primarily stained the dorsal half of the neural tube. Second, the LM staining observed within the sclerotome appeared more punctate than the FN staining.

CSAT, FN, and LM after Formation of Neural Crest-derived Ganglia

CSAT. The intensity of the detectable CSAT staining appeared to increase with embryonic age, although the pattern

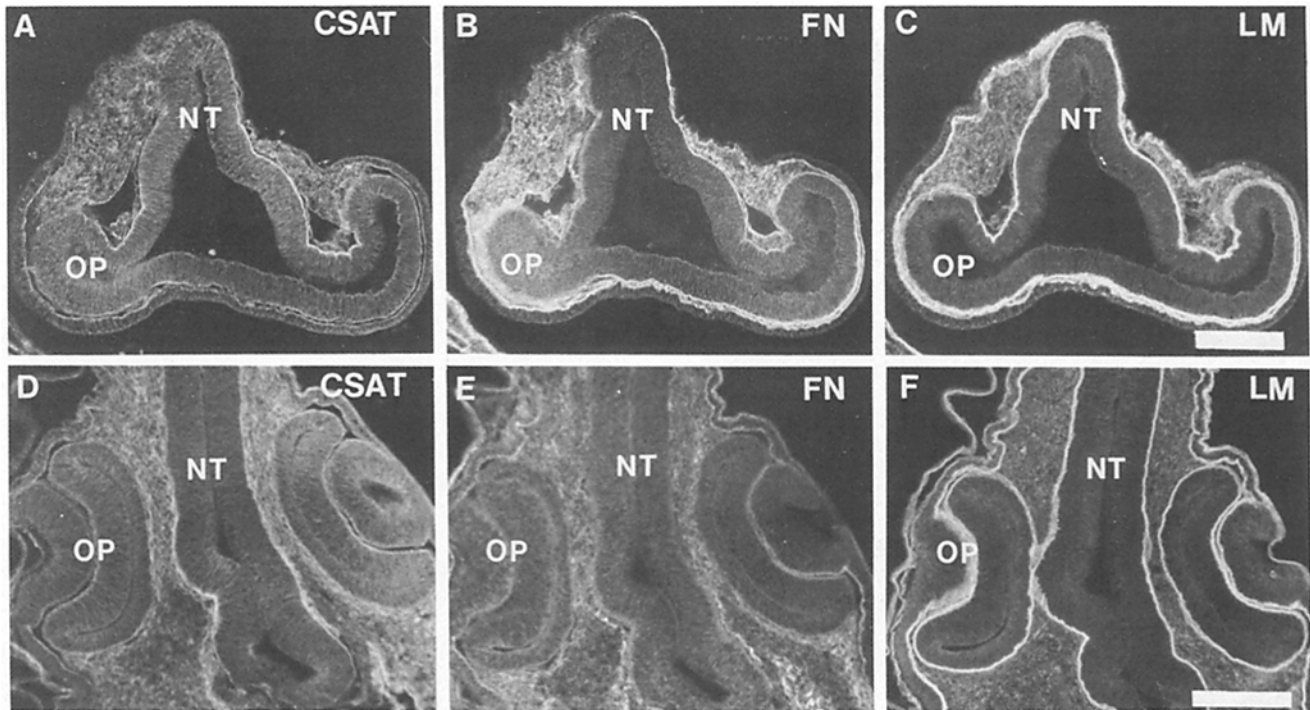*Figure 4.* Fluorescence photomicrographs of transverse sections through the rhombencephalon of Stage 13 chicken embryos showing the distribution of CSAT, *FN*, and *LM* at the level of the otic vesicles (*OP*). (*A*) CSAT was observed around cells within the neural tube (*NT*), otic vesicles, and head mesenchyme. (*B*) Low levels of FN immunoreactivity were observed around the neural tube, otic vesicles, and ectoderm, as well as within the head mesenchyme.(*C*) Strong LM immunoreactivity was observed on the basal surface of the otic vesicles, neural tube, notochord, and ectoderm; some LM was also seen in the head mesenchyme. (*D*) A control section stained with nonimmune (*NI*) serum showed no staining above background with the exception of blood cells within the dorsal aortae. Bars, 100 μm.
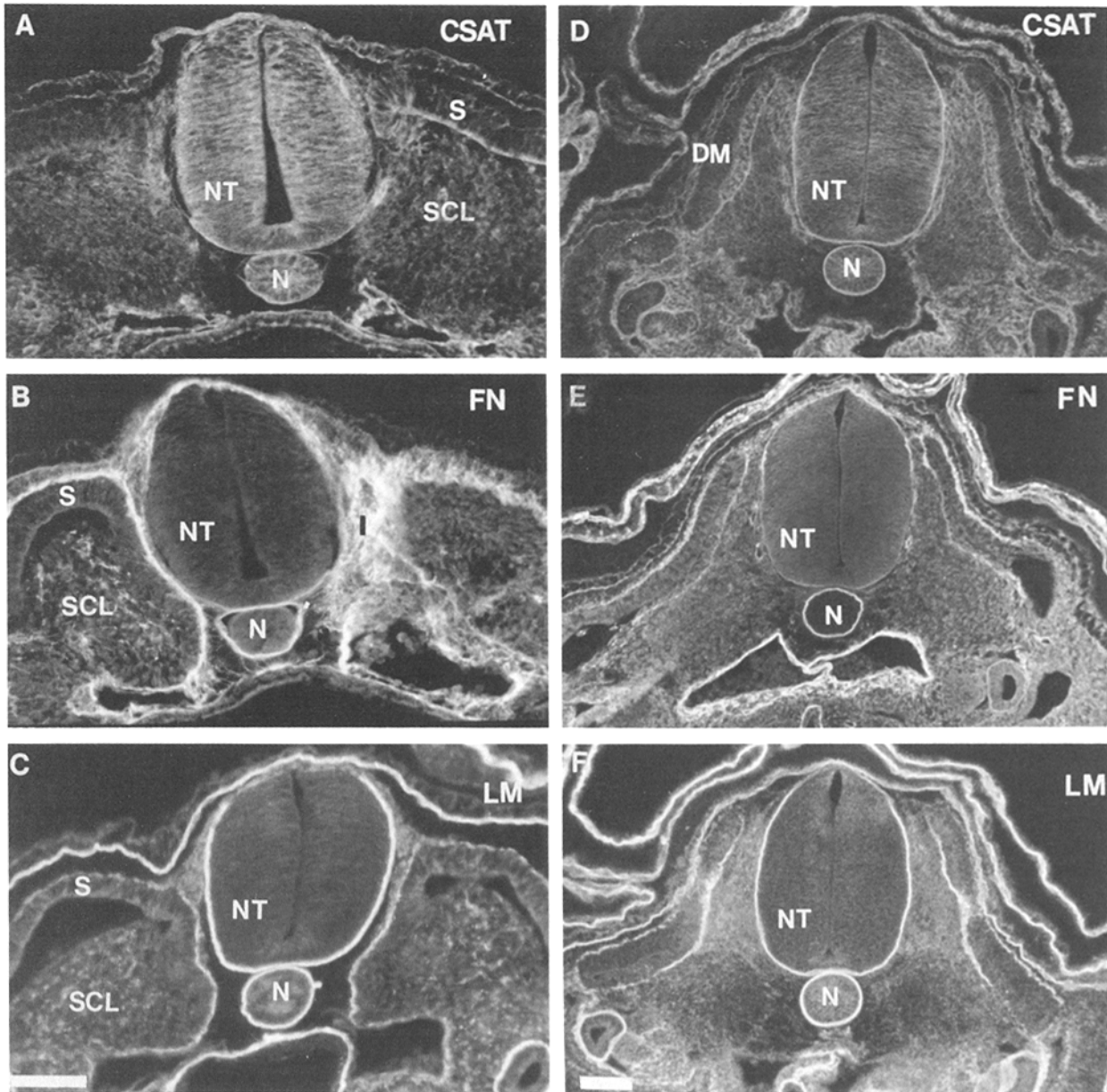
Figure 5. Fluorescence photomicrographs of transverse sections through the trunk region showing CSAT, *FN*, and *LM* immunoreactivity in the trunk region at the onset of neural crest migration (*A–C*; stage 15 embryos) and during active neural crest migration (*D–F*; stage 17 embryos). (*A*) As neural crest migration was beginning, CSAT was seen surrounding all neural tube (*NT*) cells, including the premigratory neural crest cells. CSAT was most prominent under the dermomyotomal portion of the somite (*S*) and around the dorsal aorta. Low levels of immunoreactivity were observed under the ectoderm and within the sclerotome (*SCL*); few neural crest cells have entered the sclerotome at this stage. (*B*) FN was observed around the somite (*S*), the dorsal portion of the neural tube (*NT*), and the notochord (*N*). FN immunoreactivity was particularly strong in the intersomitic space (*I*), as shown on the right side of this oblique section. Some fibrillar FN staining was noted within the sclerotome. (*C*) LM immunoreactivity was observed around the basal surface of the neural tube, notochord, ectoderm, and somite. Punctate LM staining was also observed within the sclerotome. (*D*) During active neural crest migration, the CSAT staining was more intense than in younger embryos. CSAT was observed around the basal surface of the neural tube, notochord, dermomyotome (*DM*), ectoderm, and mesonephric tubules. Within the sclerotome, CSAT immunofluorescence was distinct surrounding individual neural crest cells (*arrow*). (*E*) FN immunoreactivity was observed on the dorsal surface of the neural tube, around the dermomyotome, notochord, and dorsal aorta. Low levels of FN immunoreactivity were seen within the sclerotome through which neural crest cells migrate. (*F*) LM immunoreactivity was observed around the neural tube, notochord, ectoderm, dermomyotome, and mesonephric tubules. Low levels of FN immunoreactivity were observed within the sclerotome. Bars, 50 μm.

of staining remained relatively unchanged. As described by previous investigators (13), high levels of CSAT immunoreactivity were observed around cells within the neural crest–derived dorsal root ganglia and sympathetic ganglia.

FN. After formation of the dorsal root ganglia (DRG), the

FN immunoreactivity appeared to increase in the sclerotome in comparison with levels during the time of active neural crest migration. FN staining around epithelial structures such as the neural tube and myotome, however, appeared lower than that around epithelial structures in younger em-
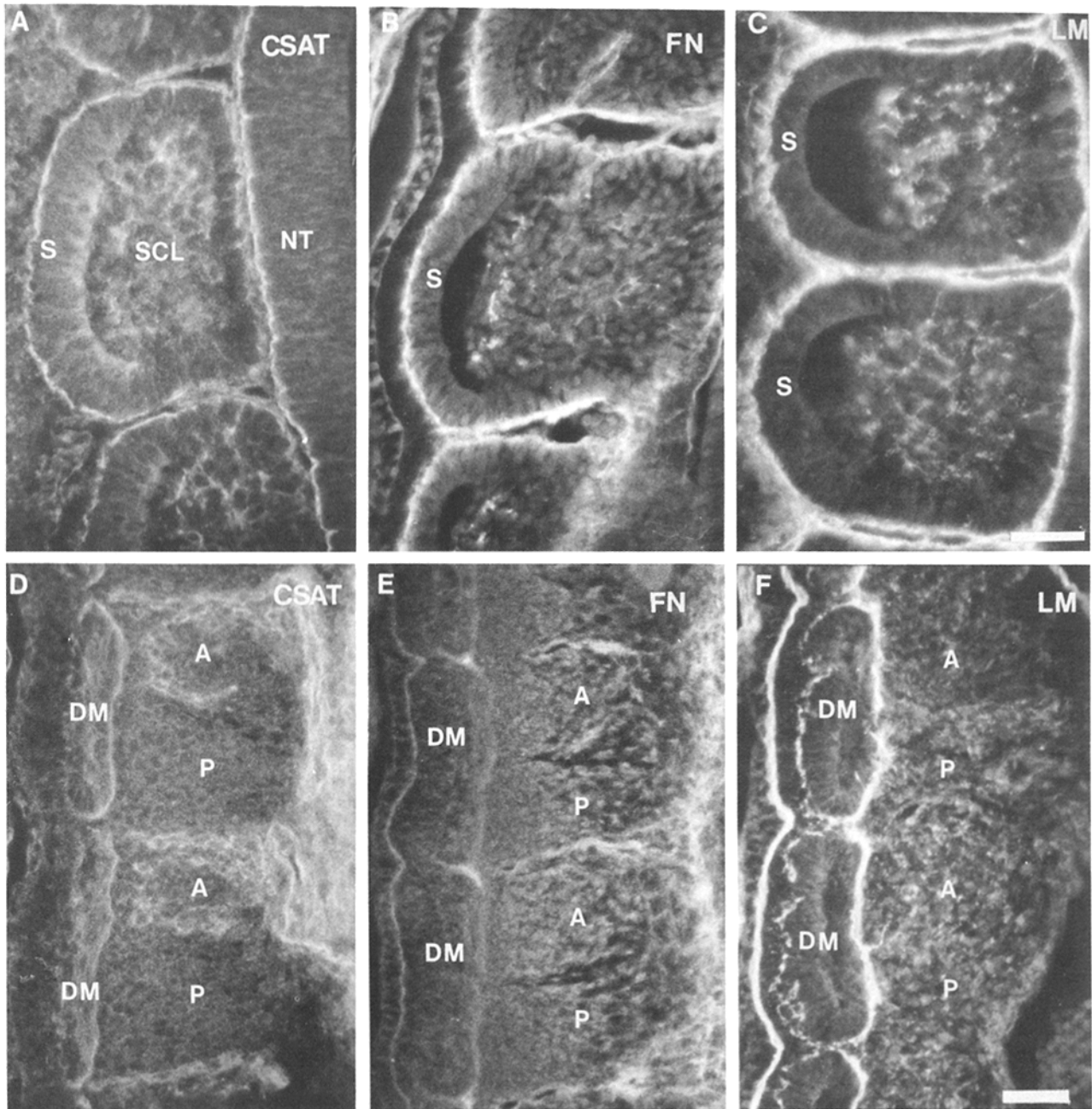
Figure 6. Fluorescence photomicrographs of longitudinal sections through the trunk region showing CSAT, *FN*, and *LM* immunoreactivity at the onset of neural crest migration (*A–C*; stage 15 embryos) and during active neural crest migration (*D–F*; stage 17 embryos). (*A*) CSAT outlined the somite (*S*) and neural tube (*NT*). Uniform staining was also observed within the sclerotome (*SCL*). (*B*) FN immunoreactivity was present around the somite. In addition, some fibrillar FN staining was seen within the sclerotome. (*C*) LM was observed around the somites, as well as in fibrillar form within the somites. (*D*) During active neural crest migration, CSAT was observed around the dermomyotome (*DM*) and surrounding neural crest cells within the anterior (*A*) half of the sclerotome. In contrast, only low levels of CSAT reactivity were observed on sclerotomal cells themselves. Consequently, the posterior (*P*) half of the sclerotome had little CSAT immunoreactivity. (*E*) FN reactivity was observed around the dermomyotome. In addition, low levels of uniform FN were seen within both anterior and posterior halves of the sclerotome. (*F*) LM immunoreactivity was observed around the dermomyotome. Within the sclerotome, uniform LM immunofluorescence was seen in both anterior and posterior halves. Bars: (*A–C*) 30 μm; (*D–F*) 50 μm.

bryos. Across from the anterior half of the somite, DRG were surrounded by FN, though only low levels of FN were detected within the ganglia. This FN distribution pattern was the reciprocal of that observed for CSAT, where DRGs had high CSAT immunoreactivity while the sclerotome had only low levels of staining.

LM. Strong LM staining outlined the forming DRG and the epithelia around the neural tube and myotome. The ganglia were relatively devoid of LM fluorescence, with the exception of a few individual cells within DRGs. The sclerotome exhibited a uniform laminin staining, which was more intense than that present in the sclerotome of younger em-

bryos. These results are in agreement with those observed by previous investigators (47).

Molecular Specificity of CSAT, FN, and LM Antibodies

The antigens recognized by the monoclonal antibodies used in this study have previously been described on tissue culture cells (1, 15, 26). In addition, CSAT has been shown to immunoprecipitate three bands from whole chicken embryos of apparent molecular masses 160, 135, and 110 kD (26). We have performed immunoblots and immunoprecipitations to ascertain if the antibodies to FN and LM recognize the same components in whole chick embryos as they do in cultures of chicken-derived cells.

The monoclonal antibody against laminin precipitated a single band of ~200 kD. This is the same molecular mass immunoprecipitated by this antibody in cultures of chick skeletal muscle and fibroblasts (1). Similarly, immunoblots using the antibody against fibronectin identified a single 220-kD band which appears identical to that reported for skeletal muscle FN (15). These data suggest that the antigens recognized by CSAT, LM, and FN antibodies are specific and show no cross-reactivity with other antigens in the whole embryo.

Discussion

The present study was designed to characterize the distribution of the CSAT antigen during early avian development and to relate this pattern to the distributions of FN and LM. The CSAT antigen is a cell surface receptor that apparently mediates the binding of some cell types to FN or LM (22). Both the cell surface receptor and its ligands in the ECM are essential elements for the formation of adhesions between the cell and the substratum. Therefore, the spatial and temporal distribution of CSAT, FN, and LM within the embryo may be important during morphogenesis. In our analysis, emphasis was placed on the stages of neural crest migration, since it has been demonstrated that normal migration of some neural crest populations is perturbed by antibodies to the CSAT receptor (4, 6). In tissue culture, both FN (40, 48) and LM (39) can serve as substrates for neural crest cell adhesion. In addition, FN (14, 34, 41, 53) and LM (47) have been detected along some neural crest migratory pathways.

Our observations suggest that the CSAT antigen is present on numerous tissues during gastrulation, neurulation, and neural crest migration. In gastrulating embryos, CSAT, FN, and LM immunoreactivities were observed on the basal surface of the epiblast, while only FN was detected on the hypoblast. In the neurulating embryo, CSAT staining was observed on many epithelial tissues including the basal surfaces of the neural folds, notochord, and ectoderm. In the cranial region, CSAT was seen around the foregut, otic, and optic vesicles. FN and LM had similar localization patterns to those of CSAT and were found in the basement membranes surrounding these structures. In the cranial mesenchyme, FN and LM were detected along the regions through which neural crest cells migrate, while CSAT was observed on the surface of cranial neural crest cells. These results suggest that CSAT is present on the surface of many epithelial cells such as the neural tube, notochord, ectoderm, and dermomyotome, as well as on mesenchymal neural crest cells; FN and LM were found in matrices surrounding these cells.

Our findings extend the recent observations of Duband et al. (13) who reported some codistribution between FN and the FN receptor during neural crest migration. At later developmental stages, other investigators have observed the CSAT/JG22 antigen on the basal surface of intestinal epithelial cells and smooth muscle (9), in many locations where FN and/or LM were also found. These observations suggest that cells containing CSAT were often in proximity to matrices containing FN and/or LM.

The parallel distributions of CSAT, FN, and LM were not, however, absolute. For example, in gastrulating tissue, the CSAT antigen was present only on the hypoblast, whereas FN was seen on both the hypoblast and epiblast. During neurulation, CSAT was found lining the basal surface of all neural tube epithelial cells whereas FN was primarily seen in the basement membrane surrounding the dorsal half of the neural tube. In both gastrulating and neurulating embryos, the CSAT distribution pattern paralleled that of LM more closely than that of FN.

In the trunk, FN and LM immunoreactivity appeared to be uniform in both anterior and posterior halves of the sclerotome. In contrast, trunk neural crest cells have previously been shown to move preferentially through the anterior half of the sclerotome (5, 45). This suggests that neither FN or LM have the selective distribution necessary to serve as a sole guiding molecule for trunk neural crest cells. The FN and LM in the sclerotome appeared fibrillar and the immunoreactivity was lower in intensity than that surrounding epithelial structures. Unlike FN or LM, the CSAT antigen was predominantly observed in the anterior half of the sclerotome. The present results together with previous observations (4, 13) indicate that the CSAT staining within the anterior somite is on the surface of neural crest cells. However, injection of JG22 (4) or CSAT antibodies (Bronner-Fraser, M., unpublished observation) into the trunk regions caused little or no perturbation in trunk neural crest migration even at concentrations tenfold higher than those causing abnormalities in the mesencephalon. These results may indicate that the receptor for FN and LM is more important in cranial than in trunk neural crest migration.

The levels of FN, LM, and CSAT immunoreactivity appeared to be dynamic at different developmental stages. In our analysis, the intensity of FN and LM immunofluorescence in the sclerotome appeared to decrease somewhat during neural crest migration and returned to higher levels after ganglion formation. The FN present around the neural tube and dermomyotome appeared to remain constant during these same times, as originally observed by Thiery et al. (49, 53). Because neural crest cells migrate through the sclerotome (5, 45) rather than between the neural tube and somites as proposed by Thiery et al. (53), our results indicate that neural crest cells may migrate at a time when FN and LM may be reduced on their migratory pathways in comparison to other developmental stages. In older embryos, LM immunofluorescence was notable around the dermomyotome, notochord, ectoderm, sclerotome, and surrounding the DRG. Only a few cells that stained with either LM or FN were detected within the ganglia. Levels of CSAT immunoreactivity were also dynamic on both epithelial and neural crest-derived tissues and appeared to increase markedly with embryonic age. In avians, development proceeds in an anterior to posterior wave. The intensity of CSAT

staining appeared graded along the rostrocaudal axis, with more developed regions showing more intense levels of immunofluorescence.

Biochemical characterization of the CSAT antigen has demonstrated that this 140-kD receptor complex can interact with both FN and LM (23). Horwitz et al. (22) have shown that a small peptide containing the amino acid sequence arg-gly-asp, responsible for the binding of fibronectin to the cell surface (43), can prevent binding of CSAT to both FN and LM. This may indicate that LM also contains an arg-gly-asp sequence. Alternatively, binding of the peptide to the CSAT antigen may alter the binding of the receptor to LM by a secondary or tertiary event; e.g., by causing a conformational change in the receptor. In light of the similarities in the distribution pattern of FN and LM in the embryo, it is interesting that both ECM molecules can interact with the same receptor complex. Thus, perturbation experiments using JG22/CSAT antibodies (4, 6) and perhaps the FN synthetic peptides (3) cannot distinguish between the functional importance of FN, LM, or possibly other yet to be identified molecules which may interact with the same receptor. These observations highlight the possibility that a number of ECM and cell surface molecules may act in concert during complex developmental events.

References

1. Bayne, E. K., M. J. Anderson, and D. M. Fambrough. 1984. Extracellular matrix organization in developing muscle: correlation with acetylcholine receptor aggregates. *J. Cell Biol.* 99:1486-1501.

2. Boucaut, J. C., and T. Darribere. 1983. Fibronectin in early amphibian embryos. Migrating mesodermal cells contact fibronectin established prior to gastrulation. *Cell Tissue Res.* 234:135-145.

3. Boucaut, J. C., T. Darribere, T. J. Poole, H. Aoyama, K. M. Yamada, and J. P. Thiery. 1984. Biologically active synthetic peptides as probes of embryonic development: a competitive peptide inhibitor of fibronectin function inhibits gastrulation in amphibian embryos and neural crest migration in avian embryos. *J. Cell Biol.* 99:1822-1830.

4. Bronner-Fraser, M. 1985. Alterations in neural crest migration by a monoclonal antibody that affects cell adhesion. *J. Cell Biol.* 101:610-617.

5. Bronner-Fraser, M. 1986. Analysis of the early stages of trunk neural crest migration in avian embryos using monoclonal antibody HNK-1. *Dev. Biol.* 115:44-55.

6. Bronner-Fraser, M. 1986. An antibody to a receptor for fibronectin and laminin perturbs cranial neural crest development in vivo. *Dev. Biol.* In press.

7. Brower, D. L., M. Wilcox, M. Poivant, R. J. Smith, and L. Reger. 1984. Related cell-surface antigens expressed with positional specificity in *Drosophila* imaginal discs. *Proc. Natl. Acad. Sci. USA.* 81:7485-7489.

8. Brown, P. J., and R. L. Juliano. 1985. Selective inhibition of fibronectin-mediated cell adhesion by monoclonal antibodies to a cell-surface glycoprotein. *Science (Wash. DC).* 228:1448-1451.

9. Chen, W.-T., J. M. Greve, D. Gottlieb, and S. J. Singer. 1985. Immunocytochemical localization of 140 kD Cell adhesion molecules in cultured chicken fibroblasts, and chicken smooth muscle and intestinal epithelial tissues. *J. Histochem. Cytochem* 33:576-586.

10. Chen, W.-T., E. Hasegawa, T. Hasegawa, C. Wienstock, and K. M. Yamada. 1985. Development of cell surface linkage complexes in cultured fibroblasts. *J. Cell Biol.* 100:1103-1114.

11. Damsky, C. H., K. A. Knudsen, and C. A. Buck. 1982. Integral membrane glycoproteins related to cell-substratum adhesion in mammalian cell. *J. Cell. Biochem.* 1:1-13.

12. Damsky, C. H., K. A. Knudsen, D. Bradley, C. A. Buck, and A. F. Horwitz. 1985. Distribution of cell substratum attachment (CSAT) antigen on myogenic and fibroblastic cells in culture. *J. Cell Biol.* 100:1528-1539.

13. Duband, J.-L., S. Rocher, W.-T. Chen, K. M. Yamada, and J. P. Thiery.

14. Duband, J. L., and J. P. Thiery. 1982. Distribution of fibronectin in the early phase of avian cephalic neural crest cell migration. *Dev. Biol.* 93:308-323.

15. Gardiner, J. M., and D. M. Fambrough. 1983. Fibronectin expression during myogenesis. *J. Cell Biol.* 96:474-485.

16. Gershoni, J. M., and G. E. Palade. 1983. Protein blotting: principles and applications. *Anal. Biochem.* 131:1-15.

17. Goodman, S., and D. F. Newgreen. 1985. Do cells show an inverse locomotory response to fibronectin and laminin substrates? *EMBO (Eur. Mol. Biol. Organ.) J.* 4:2769-2771.

18. Greve, J. M., and D. I. Gottlieb. 1982. Monoclonal antibodies which alter the morphology of cultures of chick myogenic cells. *J. Cell Biochem.* 18:221-229.

19. Hamburger, V., and H. L. Hamilton. 1951. A series of normal stages in the development of the chick embryo. *J. Morphol.* 88:49-92.

20. Hay, E. D. 1982. *In* Cell Biology of Extracellular Matrix. Plenum Publishing Corp., New York. 417 pp.

21. Heaseman, J., R. O. Hynes, A. P. Swan, V. Thomas, and C. C. Wylie. 1981. Primordial germ cells of *Xenopus* embryos: the role of fibronectin during migration. *Cell.* 27:437-447.

22. Horwitz, A. F., K. Duggan, R. Greggs, C. Decker, and C. Buck. 1985. The cell substratum attachment (CSAT) antigen has properties of a receptor for laminin and fibronectin. *J. Cell Biol.* 101:2134-2144.

23. Horwitz, R., K. Duggan, C. Buck, M. Beckerle, and K. Burridge. The CSAT antigen is a dual receptor for talin and fibronectin. *Nature (Lond.).* In press.

24. Hynes, R. O., and K. M. Yamada. 1982. Fibronectins: multifunctional modular glycoproteins. *J. Cell Biol.* 95:369-377.

25. Kleinman, H. K., F. B. Cannon, G. W. Laurie, J. R. Hassel, M. Aumailley, V. P. Terranova, G. R. Martin, and M. Dubois-Dalq. 1985. Biological activities of laminin. *J. Cell Biochem.* 27:317-326.

26. Knudsen, K., A. Horwitz, and C. Buck. 1985. A monoclonal antibody identifies glycoprotein complex involved in cell-substratum adhesion. *Exp. Cell Res.* 157:218-226.

27. Krotoski, D., and M. Bronner-Fraser. 1986. Mapping of neural crest pathways in *Xenopus laevis*. *In* New Discoveries and Technologies in Developmental Biology. H. Slavkin, editor. Alan R. Liss Inc., New York. 229-233.

28. Laemmli, U. K. 1970. Cleavage of structural proteins during the assembly of the head of bacteriophage T4. *Nature (Lond.).* 227:680-685.

29. Lander, A. D., D. K. Fuji, and L. F. Reichardt. 1985. Laminin is associated with the "neurite outgrowth-promoting factors" found in conditioned media. *Proc. Natl. Acad. Sci. USA.* 82:2183-2187.

30. Lee, G., R. Hynes, and M. Kirschner. 1984. Temporal and spatial regulation of fibronectin in early *Xenopus* development. *Cell.* 36:729-740.

31. Lesot, H., U. Kuhl, and K. Von der Mark. 1983. Isolation of a laminin-binding protein from muscle cell membranes. *EMBO (Eur. Mol. Biol. Organ.) J.* 2:861-865.

32. Liotto, L. A., P. Horan Hand, C. N. Rao, G. Bryant, S. H. Barsky, and J. Schlom. 1985. Monoclonal antibodies to the human laminin receptor recognize structurally distinct sites. *Exp. Cell Res.* 156:117-126.

33. Manthorpe, M., E. Engvall, E. Ruoslahti, F. M. Longo, G. E. Davis, and S. Varon. 1983. Laminin promotes neuritic regeneration from cultured peripheral and central neurons. *J. Cell Biol.* 97:1882-1890.

34. Mayer, B. W. Jr., E. D. Hay, and R. O. Hynes. 1981. Immunocytochemical localization of fibronectin in embryonic chick trunk and area vasculosa. *Dev. Biol.* 82:267-286.

35. McCarthy, J. B., S. L. Palm, and L. T. Furcht. 1983. Migration by haptotaxis of a Schwann cell tumor line to the basement membrane glycoprotein laminin. *J. Cell Biol.* 97:772-777.

36. Deleted in proof.

37. Malinoff, H. L., and M. S. Wicha. 1983. Isolation of a cell surface receptor for laminin from murine sarcoma cells. *J. Cell Biol.* 96:1474-1479.

38. Neff, N. T., C. Lowrey, C. Decker, A. Tovar, C. Damsky, C. Buck, and A. F. Horwitz. 1982. A monoclonal antibody detaches embryonic skeletal muscle from extracellular matrices. *J. Cell Biol.* 95:654-666.

39. Newgreen, D. F. 1984. Spreading of explants of embryonic chick mesenchymes and epithelia on fibronectin and laminin. *Cell Tissue Res.* 3236:265-277.

40. Newgreen, D. F., I. L. Gibbins, J. Sauter, B. Wallenfels, and R. Wutz. 1982. Ultrastructural and tissue-culture studies on the role of fibronectin, collagen and glycosaminoglycans in the migration of neural crest cells in the fowl embryo. *Cell Tissue Res.* 221:521-549.

41. Newgreen, D. F., and J. P. Thiery. 1980. Fibronectin in early avian embryos: synthesis and distribution along the migration pathways of neural crest cells. *Cell Tissue Res.* 211:269-291.

42. Palm, S. L., and L. T. Furcht. 1983. Production of laminin and fibronectin by Schwannoma cells: cell protein interactions in vitro and protein localization in peripheral nerve in vivo. *J. Cell Biol.* 96:1218-1226.

43. Pierschbacher, M. D., E. D. Hayman, and E. Ruoslahti. 1983. Synthetic peptide with cell attachment activity of fibronectin. *Proc. Natl. Acad. Sci. USA.* 80:1224-1227.

44. Pytela, R., M. D. Pierschbacher, and E. Ruoslahti. 1985. Identification and isolation of a 140kD cell surface glycoprotein with properties expected of

13. Duband, J.-L., S. Rocher, W.-T. Chen, K. M. Yamada, and J. P. Thiery.
1986. Cell adhesion and migration in the early vertebrate embryo: location and possible role of the putative fibronectin receptor complex. *J. Cell Biol.* 102:160-178.

a fibronectin receptor. *Cell.* 40:191–198.

45. Rickmann, M., J. W. Fawcett, and R. J. Keynes. 1985. The migration of neural crest cells and the growth of motor axons through the rostral half of the chick somite. *J. Embryol. Exp. Morph.* 90:437.

46. Rogers, S. L., P. C. Letourneau, S. L. Palm, J. McCarthy, and L. T. Furcht. 1983. Neurite extension by peripheral and central nervous system neurons in response to substratum-bound fibronectin and laminin. *Dev. Biol.* 98:212–220.

47. Rogers, S. L., K. J. Edson, P. C. Letourneau, and S. C. McLoon. 1986. Distribution of laminin in the developing peripheral nervous system of the chick. *Dev. Biol.* 113:429–435.

48. Rovasio, R., A. Delouvee, R. Timpl, K. Yamada, and J. P. Thiery. 1983. Neural crest cell migration: requirements for exogenous fibronectin and high cell density. *J. Cell Biol.* 96:462–473.

49. Ruoslahti, E., E. Engvall, and E. G. Hayman. 1981. Fibronectin: current concepts of its structure and function. *Collagen Related Res.* 1:95–128.

50. Ruoslahti, E., M. Pierschbacher, E. G. Hayman, and E. Engvall. 1982. Fibronectin: a molecule with remarkable structural and functional diversity. *Trends Biochem. Sci.* 7:188–190.

51. Sugrue, S. P., and E. D. Hay. 1982. Interaction of embryonic corneal epithelium with exogenous collagen, laminin and fibronectin: role of endogenous protein synthesis. *Dev. Biol.* 92:97–106.

52. Terranova, V. P., C. N. Rao, T. Kalebic, T. M. Margulies, and L. A. Liotto. 1983. Laminin receptor on human breast carcinoma cells. *Proc. Natl. Acad. Sci. USA.* 80:444–448.

53. Thiery, J. P., J. L. Duband, and A. Delouvee. 1982. Pathways and mechanism of avian trunk neural crest migration and localization. *Dev. Biol.* 93:324–343.

54. Timpl, R., J. Engel, and G. R. Martin. 1983. Laminin – a multifunctional protein of basement membrane. *Trends Biochem. Sci.* 8:207–209.

55. Toole, B., and R. Trelstad. 1971. Hyaluronate production and removal during corneal development in the chick. *Dev. Biol.* 26:28–35.

56. Tucker, G. C., H. Aoyama, M. Lipinski, T. Tursz, and J. P. Thiery. 1984. Identical reactivity of monoclonal antibodies HNK-1 and NC-1: conservation in vertebrates on cells derived from the neural primordium and on some leukocytes. *Cell Differ.* 14:223–230.

57. Tucker, R., and C. Erickson. 1984. Morphology and behavior of quail neural crest cells in artificial three-dimensional extracellular matrices. *Dev. Biol.* 104:390–405.